เอกสารวิชาการฉบับที่ /๒๕๕๑ Technical Paper No. /2008

การใช้ความร้อนแบบโอห์มมิคระบบต่อเนื่องเพื่อการตกตะกอนโปรตีนในน้ำล้างจากกระบวนการผลิตในอุตสาหกรรมซูริมิ

Protein Coagulation of Wash-Water from Surimi Production by Continuous Ohmic Heating System

พิสิฐ วงศ์สง่าศรี Pisit Wongsa-Ngasri

กองพัฒนาอุตสาหกรรมสัตว์น้ำ Fishery Technological Development Division
กรมประมง Department of Fisheries
กระทรวงเกษตรและสหกรณ์ Ministry of Agriculture and Cooperatives

เอกสารวิชาการฉบับที่ /๒๕๕๑

Technical Paper No. /2008

การใช้ความร้อนแบบโอห์มมิคระบบต่อเนื่องเพื่อการตกตะกอนโปรตีนในน้ำล้างจากกระบวนการผลิตในอุตสาหกรรมซูริมิ

Protein Coagulation of Wash-Water from Surimi Production by Continuous Ohmic Heating System

พิสิฐ วงศ์สง่าศรี Pisit Wongsa-Ngasri

กองพัฒนาอุตสาหกรรมสัตว์น้ำ

กรมประมง

๒๕๕๑

Fishery Technological Development Division

Department of Fisheries

2008

รหัสทะเบียนวิจัย 51-0807-51129

Table of Contents

List of Tables

List of Figures

การใช้ความร้อนโอห์มมิกแบบต่อเนื่องเพื่อการตกตะกอนโปรตีน ในน้ำล้างจากกระบวนการผลิตในอุตสาหกรรมซูริมิ

พิสิฐ วงศ์สง่าศรี*

กลุ่มนวัตกรรมผลิตภัณฑ์สัตว์น้ำเชิงพาณิชย์ กองพัฒนาอุตสาหกรรมสัตว์น้ำ กรมประมง

บทคัดย่อ

ปริมาณน้ำทิ้งต่อวันที่เกิดจากกระบวนการผลิตซูริมิมีเป็นจำนวนมากซึ่งมีปริมาณโปรตีนและค่า BOD ที่สูง และเนื่องมาจากผลการวิจัยก่อนหน้านี้พบว่า การให้ความร้อนโอห์มมิกแบบสถิตย์มีศักยภาพ ในการนำมาใช้เพื่อตกตะกอนโปรตีนในน้ำล้างเนื้อปลาทรายแดงที่ใช้ในการผลิตซูริมิได้ ดังนั้นระบบการให้ความร้อนโอห์มมิกแบบต่อเนื่องจึงถูกพัฒนาขึ้นเพื่อใช้ในการตกตะกอนโปรตีนในน้ำล้างเนื้อปลา แบบจำลอง ทางคณิตศาสตร์อันมีพื้นฐานมาจากสมการทรงพลังงานถูกพัฒนาขึ้นด้วยวิธี analytical และวิธี numerical เพื่อทำนายอุณหภูมิของน้ำล้างตลอดช่วงความยาวของโอห์มมิกเซล สารละลายเกลือความเข้มข้น 0.02 M ถูกใช้ในการทดสอบความถูกต้องแม่นยำของระบบการให้ ความร้อนโอห์มมิกแบบต่อเนื่องที่ถูกพัฒนาขึ้น ในขณะที่ น้ำล้างจากกระบวนการผลิตซูริมิที่มีการเตรียมขึ้น ใช้ทดสอบความถูกต้องแม่นยำของแบบจำลองทางคณิตศาสตร์ที่พัฒนาขึ้น โดยตัวอย่างน้ำล้างจากการผลิตซูริมิถูกเจือจางด้วยน้ำเปล่าและน้ำเกลือเข้มข้น 10% เพื่อปรับปริมาณของแข็งในน้ำล้างและค่าการนำไฟฟ้าให้เหมาะสมต่อ การทดสอบด้วยระบบโอห์มมิกที่พัฒนาขึ้น สารละลายเกลือถูกทำให้ร้อนที่ค่าความแรงของสนามไฟฟ้า 20, 25, และ 30 V/cm ณ อัตราการไหลเชิงปริมาตรของสารละลายเกลือ 75, 100, 150, และ 300 ml/min ในขณะที่น้ำล้างซูริมิผสม ถูกทำให้ร้อนที่ค่าความแรงของสนามไฟฟ้า 20, 25, และ 30 V/cm ณ อัตราการไหลเชิงปริมาตรของน้ำล้างผสม 100, 200, และ 300 ml/min ผลการทดลองจากของเหลวทั้ง สองชนิดพบว่า เมื่อให้ความร้อนในช่วงที่มีค่าความแรงของสนามไฟฟ้าสูงและอัตราการไหลเชิงปริมาตรต่ำ ซึ่งหมายถึงของเหลวได้รับความร้อนที่นานขึ้นจะทำให้ได้อุณหภูมิของของเหลวสูงกว่า ค่าอุณหภูมิที่ได้จากการคำนวณจากแบบจำลองทางคณิตศาสตร์มีค่าใกล้เคียงกับค่าที่ได้จากการทดลอง และปริมาณโปรตีน ที่เหลือในน้ำล้างจากการคำนวณจากแบบจำลองทางคณิตศาสตร์ ณ อุณหภูมิต่างๆ สอดคล้องกับค่าที่ได้จากการทดลองเช่นกัน ดังนั้น ระบบการให้ความร้อนโอห์มมิกแบบต่อเนื่องที่ถูกพัฒนาขึ้นมีความเป็นไปได้อย่างมาก ในการนำไปใช้ในการตกตะกอนโปรตีนในน้ำล้างจากกระบวนการผลิตซูริมิและยังง่ายในการควบคุม

คำสำคัญ: การให้ความร้อนแบบโอห์มมิกแบบต่อเนื่อง ซูริมิ โปรตีน การตกตะกอน น้ำล้าง

*ผู้รับผิดชอบ: เกษตรกลาง จตุจักร กรุงเทพฯ ๑๐๙๐๐ โทร: ๐-๒๙๔๐-๖๑๓๐-๔๕ ต่อ ๔๓๑๕

Email: fluke_w2001@yahoo.com

Protein Coagulation of Wash-Water from Surimi Production by Continuous Ohmic Heating System

Pisit Wongsa-Ngasri*

Fishery Technological Development Division, Department of Fisheries.

Abstract

In surimi industry, waste water is considerably generated every day with high protein content and BOD value. A continuous ohmic heating was developed and performed to coagulate protein in the wash-water after a previous study showed that a static ohmic heating has a potential to coagulate protein from fish mince (Threadfin Breams) wash-water. A mathematical model, based on the energy conservation equation, was developed by using both analytical and numerical methods to predict the temperature profiles of fluids along the length of ohmic heater. NaCl solution (0.02 M) was used to verify the accuracy of the continuous ohmic system while the prepared surimi wash-water was used to validate the accuracy of the mathematical model. The surimi wash-water samples were diluted by tap water and added with 10% NaCl to adjust its solid fraction and electrical conductivity that is suitable for testing in the developed ohmic heater. NaCl solution samples were heated under different electric field strengths (20, 25, and 30 V/cm) at different flow rates (75, 100, 150, and 300 ml/min) whereas the prepared surimi wash-water samples were heated under the same electric field strengths (20, 25, and 30 V/cm) at different flow rates 100, 200, and 300 ml/min). In all cases, heating under higher electric field strength, and lower flow rate or longer resident time, resulted in higher temperature. The predicted temperature values obtained from the relatively simple model adopted in this work complied with the values from the experiments. The remaining proteins in treated surimi wash-water samples, which were heated to different temperatures, agreed with the results from the static experiment. Therefore, the developed continuous ohmic heating system offered the promising performance and was easy to manipulate for protein recovery from surimi wash-water.

Key words: ohmic heating, continuous, surimi, protein, coagulation, wash-water

*Corresponding author: Kaset-klang Chatuchak, Bangkok 10900 Tel: 0-2940-6130-45 ext. 4315

Email:fluke_w2001@yahoo.com

Introduction

Threadfin breams (*Nemipterus spp.*) has been one of the most important raw materials in Thai surimi production recently. It was report that, in 2000, 2002, and 2003, the quantity of threadfin breams caught from the gulf of Thailand and Indian Ocean was 102, 121, and 113 thousand metric tons, respectively (Department of Fisheries, 2003; 2004; 2005). This reflects the high demand of using threadfin breams in surimi production.

However, production of surimi requires a number of washing processes, thereby not only generating a lot of wastewater which contains some proteins up to 80% (dry basis) (Lin *et al.*, 1995), but causing high BOD values as well. Conventional wastewater treatment requires long time and large digesting volume and area for treating the wastewater which might impact the production capacity and productivity if land resource is limited. Furthermore, if proteins can be partially or considerably removed from the waste water before entering treatment system, BOD value will substantially decrease and cost of water treatment then will be significantly reduced, consequently decreasing of total capital cost. Also, if the recovered proteins are somehow utilized, for instance, to additionally use in surimi based products for low market or pet food, this will finally decrease processors' cost. Consequently, any innovative method for wastewater treatment would be preferable.

Ohmic heating is a promising method since there are many advantages of ohmic heating over conventional heating in terms of more energy efficiency (86-96 %) (Huang *et al*., 1997); higher heating rate; more compact system, and no requirement for large production area It has been studied in several applications (Wongsa-Ngasri, 2004) and it was also studied to coagulate protein of wash-water from surimi production by using static ohmic system (Wongsa-Ngasri, 2007). He reported that ohmic heating at final temperature of 70^{o}C could reduce protein content, COD value, BOD value, TS, and TDS 58.10%, 74.97%, 76.58%, 56%, and 38.91% of those before ohmically heated, respectively. However, the ohmic study was set up in static system which can not or is difficult to be applied in commercial and industrial scale. Studying a continuous lab-scale ohmic system might shred the light to increase a potential of using ohmic heating as an alternative wastewater treatment for Thai surimi production plant especially for small and medium size factory.

Objectives

1. To design and invent a lab-scale continuous ohmic heating system for possibility of using it to coagulate proteins in fish mince (threadfin breams) wash-water
2. To develop a simple mathematical model for predicting temperatures of surimi wash-water at steady state condition during ohmic heating in the developed system
3. To Validate the accuracy of the ohmic system and mathematical model

Materials and Methods

I. Continuous Ohmic Heating System Setup

Schematic diagram of a continuous ohmic system shown in Figure 1 consisted of an ohmic cell, an ordinary manual on-off variable transformer (0-240 Volts), a digital recordable power meter (Yokogawa model WT110), and a data logger (Yokogawa model DR 610), a screw pump, a supply tank, a recycle tank, and a collecting tank. As seen from Figure 2, the ohmic cell made from an acrylic tube was 700 mm long, and 14 mm in the internal diameter. Six cylindrical 316 stainless steel electrodes were lined in series with a constant interval of 80 mm between each other. The flow rate-controllable pump and ball valve were used to adjust the flow rate of the wash-water (75, 100, 150, 200 and 300 ml/min) to be heated. The variable transformer was used to control voltage, resulting in generating the desired electric field strengths (20, 25 and 30 V/cm), and the digital meter was used to record the voltage across the cell and the electric current every 10 seconds.

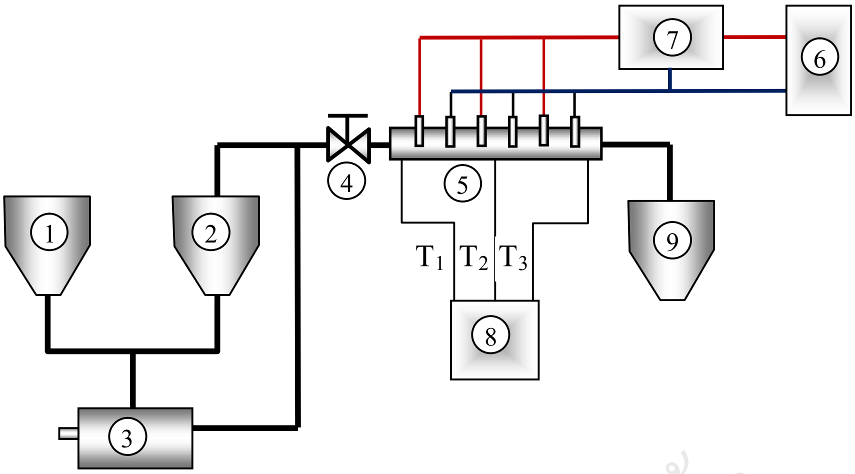

Figure 1: Schematic diagram of the continuous ohmic heating system. 1, 2, 9: the supply, recycle and collecting tank, respectively; 3: the screw pump; 4: the ball valve; 5: the continuous ohmic cell; 6: the variable transformer; 7: the digital power meter; 8: the data logger

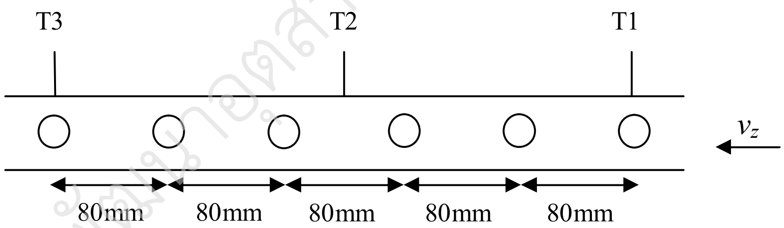

Figure 2: Diagram of the designed continuous ohmic cell

II. Mathematical Model Development

The continuous ohmic heating system was developed based on the one dimentional energy conservation equation and assumed that the electric field was uniform and there were no energy loss and heat conduction in fluid phase as well as the fluid flow in the device was plug flow. The temperature profile of the fluid in the ohmic heater could be written in equation (1) (Sastry, 1992).

$$\frac{\sigma.E^2}{1000} = \rho.C_p.v_z.\frac{\partial T}{\partial z} \qquad (1)$$

The specific heat (C_p) and the density (ρ) of the surimi wash-water were approximately estimated as 4.18 kJ/kg.^{o}C (Heldman and Singh, 1981) and 1000 kg/m^3, respectively.

Analytical and Numerical Methods

Two methods of solving equation (1) are conducted in this work, analytical and numerical method. The analytical method can be directly integrated from the equation (1) when simple relationship of fluid electrical conductivity as a function of temperature is known whereas the numerical method, for the case of more complex function, adapted from the work of Sastry (1992) is more suitable.

III. Validation the Accuracy of the Ohmic System and Mathematical Model

Solution of 0.02 M NaCl and surimi wash-water were used as fluid samples in the experiments. The NaCl solution and the surimi wash-water were used to verify the accuracy of the developed ohmic heating system and the developed mathematical model, respectively, by comparing the experimental temperature data-running at different flow rates with three designed electric field strengths (20, 25 and 30 V/cm) - with the predicted values by using the proposed mathematical model from both analytical and numerical method.

Surimi Wash-Water Collection and Preparation

The fish mince wash-water was obtained from a surimi production plant in Samuthsakorn province (Seven lots of the wash-water). Whole threadfin breams were headed, gutted, washed, and minced through the meat-bone separator before being washed in the first washing tank, which contained high protein content, and subsequently dewatered and washed in other washing tanks. In this experiment, the wash-water from the last washing tank was collected, filled in plastic bottles, and kept cooled in a foam box containing ice during transportation to the laboratory. The experiment was performed within two hours after the sample was collected. The concentration of NaCl contained in the wash-water ranged from 0.3% to 0.5% (w/v).

Surimi wash-water samples were then diluted with tap water. The main objective of the dilution was to minimize the effect of protein fouling at the electrode surface during ohmic heating since the ohmic cell was relatively small (lab scale). The dilution, however, did not necessitate in an industrial scale because the problem can be avoided by adjusting the fluid flow rate and increasing the length of the ohmic cell. In order to compensate the effect of the dilution, resulting in decreasing of the electrical conductivity, some 10% NaCl solution was added to the diluted surimi wash-water. After the preliminary test, an optimum ratio among the amount of surimi wash-water, tap water, and 10% NaCl solution for the developed device in this study was found to be 20:60:3 by volume, respectively.

(1) Measurement of the Electrical Conductivity as Function of Temperature

The measurement of the electrical conductivity were applied on both types of fluids by using a static ohmic heating system in order to receive relationships of the electrical conductivity of both fluids as a function of temperature which is the necessary information for predicting temperatures in the proposed mathematical model. The static system consisted of a T-ohmic cell, a variable transformer (0-240 Volts), a digital recordable power meter (Yokogawa model WT110), and a data taker (Yokogawa model DR 610). The T-ohmic cell was made from an acrylic tube having the length and the internal diameter of 300 mm and 50 mm, respectively. Two disc-shaper 316L stainless steel electrodes, 2 mm thick and 50 mm in diameter, were fixed at both ends of the cell with 75 mm of the gap distance. The variable transformer was used to control voltage, generating the desired electric field strength (20, 25 and 30 V/cm), and the digital meter was used to record the voltage across the cell and the electric current every 10 seconds.

The sample of 170 mL was filled into the cell. The air bubbles were carefully removed to ensure the precision of electrical conductivity measurement. The sample was then heated at the electric field strengths (20, 25, and 30 V/cm) until reaching the desired temperatures (70 ^{o}C or higher). The temperature, voltage and current were recorded every 10 seconds. With the assumption that there is no voltage drop across the wiring and connectors in the circuit, the electrical conductivity of the fluids can be calculated by using equation (2) (Palaniappan and Sastry , 1991a, b):

$$\sigma = \frac{I}{V} \cdot \frac{L}{A} \qquad (2)$$

(2) Comparison between Temperatures of NaCl Solution and Surimi Wash-Water from Experiments and Those Predicted from the Developed Mathematical Model

The ohmic system accuracy was verified by data comparison from NaCl solution and the accuracy of the mathematical model was validated by those from surimi wash-water. During heating experiment the temperatures at steady state of the fluid samples were measured and compared to the predicted values obtained from using both analytical and numerical methods.

(3) Remaining Protein Comparison

Moreover, the amount of the remaining protein in the treated surimi wash-water were compared to those reported in the static ohmic heating experiment of Wongsa-Ngasri (2007) which were analyzed by using Kjeldahl method with the conversion factor of 6.25 according to AOAC standard methods (Cunniff, 1995).

Results and Discussion

I. Continuous Ohmic Heating System Setup

The invented continuous ohmic cell, variable transformer, and digital power meter were shown in Figure 3 and 4 while the continuous ohmic heating system was in Figure 5.

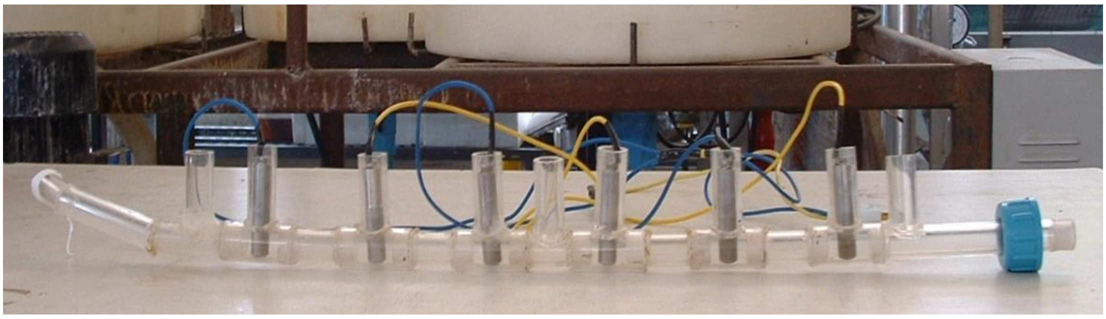

Figure 3: The Continuous Ohmic Cell Invented

(a) (b)

Figure 4: (a) Variable Transformer and (b) Digital Power Meter Used in the Continuous Ohmic Heating System

Figure 5: The Continuous Ohmic Heating System

II. Mathematical Model Development

Method I. Analytical method

Palaniappan and Sastry (1991a, b) reported that the electrical conductivity of the fluid samples had the linear relationship with the temperature as equation (3):

$$\sigma = a.T + b \tag{3}$$

Assuming that all other physical properties of the samples are constant over a range of the testing temperatures, by substitute the electrical conductivity value from equation (3) into equation (1) and then integrating, the solution becomes:

$$T(z) = \frac{1}{a}\left[(aT(0) + b).\exp\left(\frac{aE^2 z}{1000\,\rho C_p v_z}\right) - b \right] \tag{4}$$

The equation (4) can be used to calculate the temperature of fluid in any location (z) along the continuous ohmic cell if the applied electric field strength and flow rate are given.

Method II. Numerical method

The estimation of temperature *T(z)* was adapted from the method described in Sastry (1992). The procedure can be summarized as following steps:

1. Divide the chamber of the continuous ohmic cell into *n* small sections. Thickness of each section, represented by *dz*, is therefore equals to total length of heating section (L) divided by *n*. The electric field strength "E_i" is firstly assumed to be *V/L* for all sections. Then, we can draw the model geometry as presented in Figure 6.

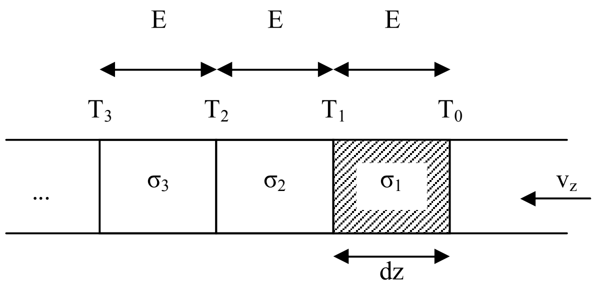

Figure 6: Model geometry of the heating chamber of the continuous ohmic cell

2. Estimate the temperature in any incremental section T_{i+1} based on equation (1) by using the following equation:

$$\frac{\sigma_i.(E_i)^2}{1000} = \rho.C_p.v_z\left(\frac{T_i - T_{i-1}}{dz}\right) \tag{5}$$

Once the inlet temperature of fluid T_0 is known, it is possible to calculate the temperature T_1, T_2, .., T_n. The electrical conductivity of each section, σ_i, is obtained using equation (3), and the average temperature value, $(T_i+T_{i-1})/2$ is used in the calculation of σ_i.

3. Estimate total resistance "R" from the summation of the resistance of each individual section (equation (6)) where the resistance of section i, R_i, is calculated by using equation (7).

$$R = \sum_{i=1}^{n} R_i \tag{6}$$

$$R_i = \frac{L}{\sigma_i.A} \tag{7}$$

4. Estimate the electric current, "I", as equation (8).

$$I = \frac{V}{R} \tag{8}$$

5. Recalculate the electric field strength across each section, "E_i", as equation (9)

$$E_i = \frac{I.R_i}{dz} \tag{9}$$

6. Repeat step 2-5 until the temperature of each individual section converged.

III. Verification the Accuracy of the Ohmic System Using NaCl Solution

(1) Measurement of the Electrical Conductivity of NaCl Solution and Surimi Wash-Water

The electrical conductivity of NaCl solution was examined by using the static ohmic heating device. The temperature dependence equation of electrical conductivity was determined. Linear relationship between the electrical conductivity and temperature was found and presented in equation (10) which was well agreed with the results reported by Sukprasert (1999) which studied with various concentrations of NaCl solution.

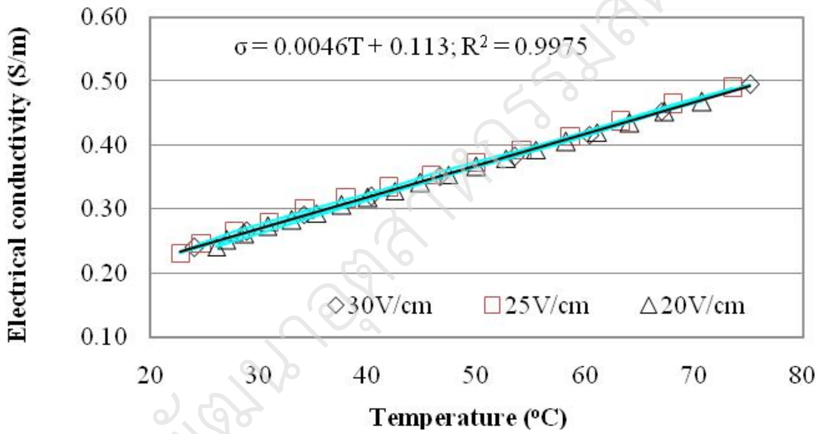

Figure 7: Electrical conductivity of 0.02M NaCl Solution

$$\sigma = 0.0046T + 0.113;\ R^2 = 0.9975 \tag{10}$$

The electrical conductivity of the diluted surimi wash-water was analyzed by using the static ohmic heating device as same method as was that of the NaCl solution. The relation between the electrical conductivity and temperature was presented in the following equation:

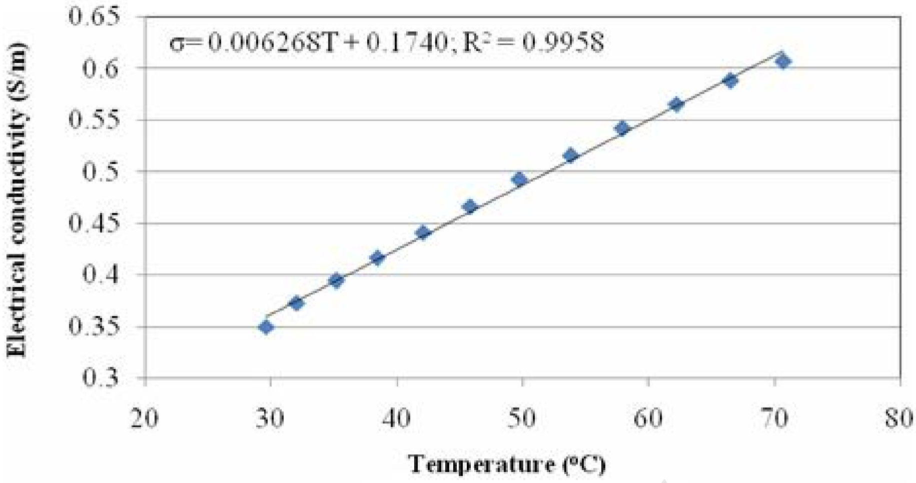

Figure 8: Electrical conductivity of the surimi wash-water diluted with tap water and 10% NaCl solution (ratio 20:60:3 by volume)

$$\sigma = 0.0063T + 0.1740;\ R^2 = 0.9958 \qquad (11)$$

(2) Comparison between Temperatures of NaCl Solution and Surimi Wash-Water from Experiments and Those Predicted from the Developed Mathematical Model

Table 1 shows the temperature of the NaCl solution measured during heating in the lab-scale continuous ohmic heater by using different conditions of treatments. At a higher flow rate of the solution, the more accurate predicted temperatures could be observed. However, at a lower flow rate, the effect of heat conduction in fluid phase along the heater outlet to the inlet direction on the temperature became more significant than at a higher flow rate. Therefore, the temperatures measured from the experiment were higher than the predicted values. At a high flow rate, the heat convection overcame the heat conduction mode, and the predicted values became closer to the temperatures measured from the experiment.

Table 1: Temperatures of 0.02M NaCl solution measured at different conditions compared with the predicted values by using analytical method (Method I) and numerical method (Method II)

Flow Rate (ml/min)	EFS[a] (V/cm)	Temperature (^{o}C)						
		T1[b]	T2[c]			T3[d]		
		Exp[e]	Exp[e]	Method I	Method II	Exp[e]	Method I	Method II
300	20	27.3	28.7	29	29.1	30.3	30.8	30.8
	25	27.3	29.7	30	30.1	32.2	32.8	32.8
	33	26.8	32.0	31.4	31.6	35.9	36.4	36.2
150	20	26.4	29.8	29.8	30.0	33.8	33.4	33.4
	25	25.8	30.9	31.2	31.5	36.4	37.1	37.1
	30	25.4	33.3	33.2	33.7	43.0	42.3	42.3
100	20	26.9	32.5	32.1	32.4	38.3	37.9	37.9
	25	27.6	37.2	36.2	36.7	46.9	46.1	46.1
	32	27.6	46.6	42.3	43.4	64.3	61.3	61.4
75	20	27.5	35.2	34.7	35.0	43.2	42.9	42.7
	25	28.3	41.8	40.2	40.9	54.8	54.7	54.7
	30	29.3	52.3	47.5	48.6	75.6	72.0	71.9

[a] Electric field strength.

[b,c,d] The temperatures at z=0 (entrance), 0.2 m (middle), and 0.4 m (exit) (see Figure 2).

[e] The temperature measured from the experiment.

However, the surimi wash-water contains protein and will coagulate during ohmic heating, causing the possibility of the protein accumulation if the flow rate is not high enough to generate convection force that could convey the solid out of the cell. The accumulated solid will act as an insulator that affects the heating rate of the system. From the preliminary test, the flow rate of 75 ml/min was too low to generate the required force. Therefore, in the surimi wash-water experiment, the low flow rate of 75 ml/min would not be performed. And to make it simpler, the flow rate of 100, 200, and 300 mL/min were used.

Then, the continuous ohmic heating experiments of prepared surimi wash-water samples were performed under 3 levels of electric field strength (20, 25, and 30 V/cm) at 3 different flow rates (100, 200, and 300 ml/min). The results from both experiment and model prediction are shown in Table 2.

Table 2: Temperatures of samples that were measured from the experiments and predicted by using analytical method (Method I) and numerical method (Method II).

Flow Rate (ml/min)	**EFS[a] (V/cm)**	**Temperature (°C)**						
		T1[b]	**T2[c]**			**T3[d]**		
		Exp[e]	**Exp[e]**	**Method I**	**Method II**	**Exp[e]**	**Method I**	**Method II**
300	20	28.3	30.1	30.8	30.9	32.7	33.4	33.3
	25	28.4	33.1	32.3	32.6	36.9	36.5	36.5
	30	28.5	34.3	34.3	34.5	40.0	40.6	40.5
200	20	28.9	32.9	32.7	32.9	36.8	36.8	36.7
	25	29.2	36	35.3	35.6	43.1	42	41.9
	30	29.5	39.8	38.7	39.0	50.1	49.4	48.8
100	20	29.7	38.8	37.7	38.1	47.3	46.8	46.6
	25	29.9	46.3	42.9	43.6	58	58.8	58.6
	30	30.3	56.9	50	51.5	70.4	76.5	76.7

[a] Electric field strength.

[b,c,d] The temperatures at z=0 (entrance), 0.2 m (middle), and 0.4 m (exit) (see Figure1).

[e] The temperature measured from the experiment.

At a high flow rate, the temperature prediction from the model showed the same trend as those found in the case of 0.02 M NaCl solution which was more accurate results than at a low flow rate. When the wash-water samples were heated at 30 V/cm with the flow rate of 100 ml/min or lower, it was found that there was the accumulation of protein solids only at the last electrode near the exit of the ohmic cell due to the fluid temperature near the exit was high enough to coagulate protein which was around 60-70 °C, Therefore, it can be expected that 50-60% of the protein contained in the sample is coagulated at the mentioned location. It seems that low flow rate cannot generate enough convective force to carry the coagulated protein through the exit of the cell. Some of the protein solids loosely contacted with the electrode and increasingly accumulated. Therefore, it was possible that the solids played a role as an insulating material, thereby decreasing overall electrical conductivity as suggested by Guérin *et al*. (2007). Consequently, the heating rate of the fluid decreased and its temperature at the position T3 was lower than the predicted-from-model values. Moreover, the protein solids possibly created the pressure drop that could decrease the flow rate and increased the resident time. So the temperature of the surimi wash-water samples at the middle of the cell became higher than the predicted values. Although there are still some differences between the actual and predicted temperatures, the applied models are quite simple and provide adequate accuracy.

Nevertheless the system performance can be improved by: 1) operating the system at an appropriate flow rate together with increasing the electric field strength and heating chamber length will help to prevent the protein solid accumulation; 2) using of the cross field ohmic cell, as described by Vincente *et al*. (2006), should facilitate the solid flow.

(3) Remaining Protein Comparison

Figure 9 shows the plot of the remaining proteins after heating to different temperatures. The results confirmed that no differences between the remaining proteins in the surimi wash-water sample heated by using the static (Wongsa-Ngasri, 2007) and continuous ohmic heating system. Consequently, the sample temperature is the key parameter of protein recovery from the surimi wash-water no matter what system is implemented.

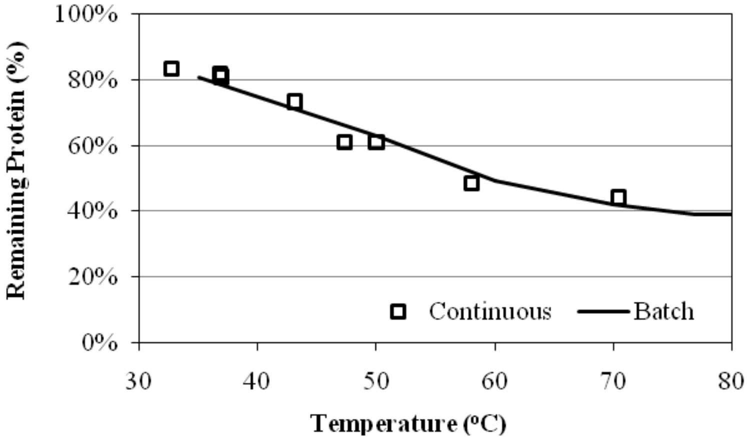

Figure 9: The remaining proteins in the sample after heating to different temperatures using the continuous ohmic heating system and compared with the result obtained using the batch ohmic heating system (Wongsa-Ngasri, 2007).

Conclusions

A simple proposed mathematical model solved by either analytical or numerical methods showed good temperature prediction of both 0.02M NaCl solution and surimi wash-water under the continuous ohmic heating system. The temperatures of the fluid obtained from both the experiment and model prediction increased with the electric field strength but decreased with the flow rate. The model gave better prediction of the fluid temperature at higher flow rate, where heat convection overcame fluid phase heat conduction, than at a lower flow rate, where heat convection had less influence. Overall, the developed continuous ohmic heating system offers adequate performance and is controllable in order to obtain a desired heating temperature for protein recovery from surimi wash-water.

Acknowledgement

The authors would like to give special thanks to Department of Food Engineering, Faculty of Engineering, King Mongkut's University of Technology for the laboratory support of this work.

Nomenclatures

A	cross sectional area (m^2)
a, b	arbitrary constants
C_p	specific heat (kJ/kg.^{o}C)
E	electric field strength (V/m)
L	length (m)
I	electric current (A)
n	number of the small sections
R	resistance (Ω)
T	temperature at distance z from the inlet (^{o}C)
V	voltage drop (Volts)
v_z	velocity in (m/s)
ρ	density (kg/m^3)
σ	electrical conductivity (S/cm)

References

Cunniff, P. 1995. Official Methods Of Analysis of AOAC International Volume 1, agricultural chemicals; contaminants; drugs, 16th ed. Arlingtion. pp.8-9.

Department of Fisheries. 2005. Statistics of Fishery Production, 2003, Fisheries Statistics of Thailand 2003. No. 6/2005. p.32.

Department of Fisheries. 2003. Statistics of fishery production, 2000, Fisheries Statistics of Thailand 2000. No. 4/2003. p.32.

Department of Fisheries. 2004, Statistics of Fishery Production, 2002, Fisheries Statistics of Thailand 2002. No. 30/2004. p.32.

Guérin, R., G. Ronse, L. Bouvier, P. Debreyne, and G. Delaplace. 2007. Structure and rate of growth of whey protein deposit from *in situ* electrical conductivity during fouling in a plate heat exchanger. *Chemical Engineering Science*. 62:1948–1957

Heldman, D.R. and R.P. Singh. 1981. Food Process Engineering. Saybrook Press, Connecticut.

Huang, L., Y. Chen and M. T. Morrissey. 1997. Coagulation of fish protein from frozen fish mince wash water by ohmic heating. *J. of Food Proc. Eng*. 20(4): 285 – 300.

Lin, T. M., J. W. Park and M. T. Morrissey. 1995. Recovered protein and reconditioned water from surimi processing waste. *J. Food Sci*. 66: 4-9

Liphard, K.G., A. Jost and G.M. Schneider. 1976. Determination of the specific heat capacities of aqueous sodium chloride solutions at high pressure with the temperature jump technique. *Journal of Physical Chemistr*. 81(6):547-550.

Palaniappan, S. and S. K. Sastry. 1991a. Electrical conductivity of selected solid foods during ohmic heating. *J. Food Proc. Eng*. 14: 221 – 236.

Palaniappan, S. and S .K. Sastry. 1991b. Electrical conductivity of selected juices: influences of temperature, solid content, applied voltage, and particle size. *J. food Proc. Eng*. 14: 247 – 260.

Sastry, S.K. 1992. A Model for heating of liquid-particle mixtures in a continuous flow ohmic heater. *Journal of Food Process Engineering*. 15: 263-278.

Sukprasert, A., 1998. Electrical conductivity property of foods for ohmic heating application. The Degree of Master Thesis. Food Engineering Department, Faculty of Engineering, King Mongkut's University of Technology Thonburi.

Vicente, A.A., I. Castro, and J.A. Teixeira. 2006. Ohmic Heating for Food Processing. In D.W. Sun (Ed.), *Thermal Food Processing.* CRC Press, New York.

Wongsa-Ngasri, P. 2007. Protein Coagulation of Wash-Water from Surimi Production by Ohmic Heating Part 1: Static Ohmic Heating System. Technical Paper No. 1/2007. Fishery Technological Development Division. Department of Fisheries.

Wongsa-Ngasri, P. 2004. Ohmic heating of biomaterials: peeling and effects of rotating electric field. Ph.D. dissertation. The Ohio State University.

Appendix

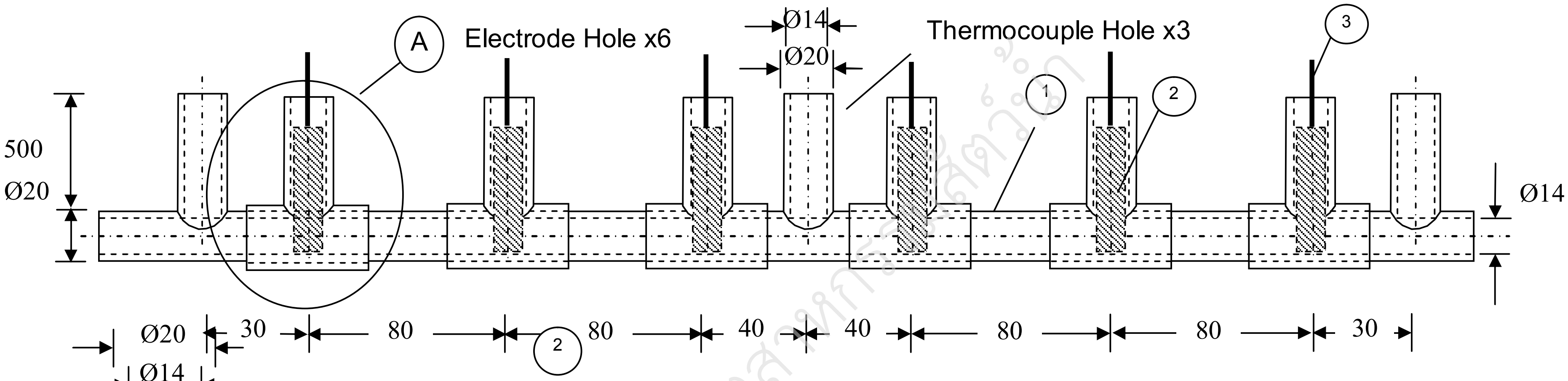

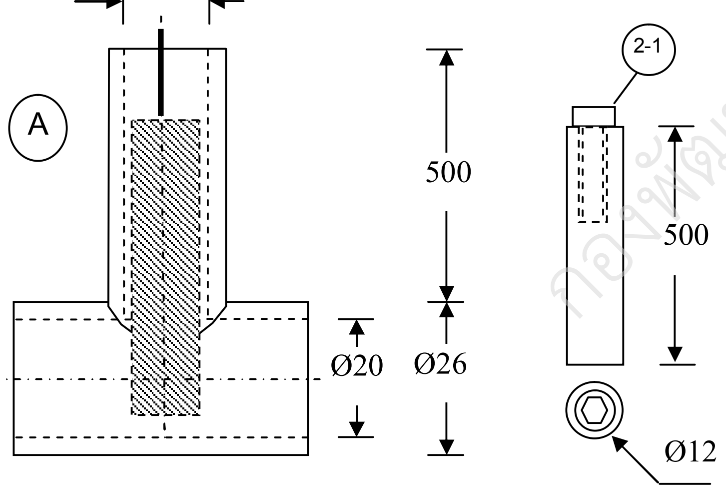

Number	Part Name	Material	Quantity
1	Cell body	Acrylic	1
2	Electrode	Stainless 316	6
2-1	Bolt M6	Stainless	6
3	Wire	Copper	6

Figure 1: Drawing of Continuous Ohmic Cell and Its Components (in mm)

2. การออกแบบชุดให้ความร้อนโอห์มมิคแบบต่อเนื่อง

ชุดให้ความร้อนโอห์มมิคแบบต่อเนื่องนี้ ได้รับการออกแบบโดยอาศัยข้อมูลจากการทดลองให้ความร้อนโอห์มมิคแบบสถิตย์ ค่าความเข้มสนามไฟฟ้าที่ใช้มีค่า 20, 25 และ 30 โวลท์/เซนติเมตร และหม้อแปลงที่เลือกใช้มีกำลังสูงสุดเท่ากับ 1000 โวลท์-แอมป์ แรงดัน 0-260 โวลท์ วางแท่งอิเลคโทรดเรียงกันแบบอนุกรมเพื่อสร้างสนามไฟฟ้าเป็นระยะๆ รวมทั้งสิ้น 5 ช่วง การต่ออิเลคโทรดแบบนี้มีข้อดีคือทำให้สามารถลดขนาดแรงดันไฟฟ้าไม่ให้สูงมากนักทำให้เกิดความปลอดภัยในการทำงาน สามารถต่อปรับช่วงให้ความร้อนได้ง่ายโดยปรับจำนวนอิเลคโทรดที่เหมาะสม และ ต้นทุนอุปกรณ์ถูกเพราะไม่ต้องใช้หม้อแปลงแรงดันสูงเป็นแหล่งกำเนิดพลังงาน

กำหนดแรงดันไฟฟ้าสูงสุดที่ใช้ในการสร้างสนามไฟฟ้าเท่ากับ 240 โวลท์ เพื่อให้ได้ความเข้มสนามไฟฟ้าขนาด 30 โวลท์/เซนติเมตร จะได้ระยะห่างระหว่างอิเลคโทรด L=0.08 เมตร/ช่วง จำนวน 5 ช่วง จะได้ระยะทางทั้งหมดในการให้ความร้อน = 5xL = 0.4 เมตร

ค่าความนำไฟฟ้าของน้ำล้างปลาบดที่อุณหภูมิ 20 องศาเซลเซียส: $1.4 < \sigma_{20} < 2.6$ (ซีเมนส์/เมตร) และช่วงอุณหภูมิทำงานของระบบให้ความร้อน 20-70 องศาเซลเซียส ในการออกแบบจะใช้ค่าการนำไฟฟ้าสูงสุดคือ σ_{20} เท่ากับ 2.6 ซีเมนส์/เมตร

จากการทดลองภาคสถิต สามารถทำนายความสัมพันธ์ระหว่างค่าการนำไฟฟ้าและอุณหภูมิได้จากสมการ 4.3

$$\sigma^* = 0.4485.T^*$$

โดย $\sigma^* = \sigma/\sigma_{20} - 1$ และ $T^* = T/20 - 1$

แทนค่า σ_{20} เท่ากับ 2.6 ซีเมนส์/เมตร จะได้

$$\sigma = 0.0063T + 0.1330$$

(ก.6)

จากสมการพลังงานตามสมการที่ 3.5

$$T(z) = \frac{(aT_i + b).e^{\frac{a(\nabla V)^2 z}{1000 \rho C_p v_z}} - b}{a} \qquad \text{(ก.7)}$$

แทนค่า

z = 0.4 เมตร

a = 0.0063 ซีเมนส์/(เมตร-องศาเซลเซียส)

b = 0.1330 ซีเมนส์/เมตร

T_i = 30 องศาเซลเซียส (ประมาณอุณหภูมิห้อง)

T(0.4) = 70 องศาเซลเซียส

V=3000 โวลท์/เมตร

จะได้ความเร็วของน้ำทิ้งที่ต้องการ $v_z = 0.0094$ เมตร/วินาที และสามารถคำนวณอุณหภูมิที่ตำแหน่งต่างๆ ที่อิเลคโทรดได้ดังนี้

อิเลคโทรดตัวที่ 1: z=0 (ทางเข้า)	T1	= 30 องศาเซลเซียส
อิเลคโทรดตัวที่ 2: z=0.08 เมตร	T2	= 36 องศาเซลเซียส
อิเลคโทรดตัวที่ 3: z=0.16 เมตร	T3	= 43 องศาเซลเซียส
อิเลคโทรดตัวที่ 4: z=0.24 เมตร	T4	= 51 องศาเซลเซียส
อิเลคโทรดตัวที่ 5: z=0.32 เมตร	T5	= 60 องศาเซลเซียส
อิเลคโทรดตัวที่ 6: z=0.40 เมตร (ทางออก)	T6	= 70 องศาเซลเซียส

เมื่อทราบอุณหภูมิในแต่ละจุดแล้ว สิ่งที่ต้องหาต่อไปคือขนาดหรือเส้นผ่านศูนย์กลางของเซลล์ที่เหมาะสม เซลล์ขนาดใหญ่ต้องการกำลังไฟฟ้าที่จะจ่ายให้แก่ระบบสูงกว่าเซลล์เล็กเนื่องจากเซลล์ใหญ่มีความต้านทานไฟฟ้าต่ำกว่าเซลล์เล็กนั่นเอง รูปที่ ก-4 และ ก-5 แสดงภาพจำลองเซลล์ที่สร้างขึ้น เมื่อพิจารณาบริเวณระหว่างอิเลคโทรดตัวที่ 1 และตัวที่ 2 สามารถหาความต้านทานที่ตำแหน่ง l ใดๆที่มีความหนา dl ได้ดังนี้

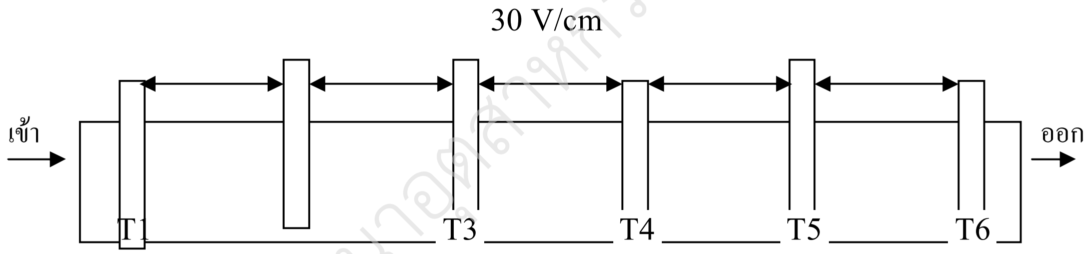

รูปที่ ก-4 ภาพจำลองเซลล์ของระบบให้ความร้อนโอห์มมิคแบบต่อเนื่อง

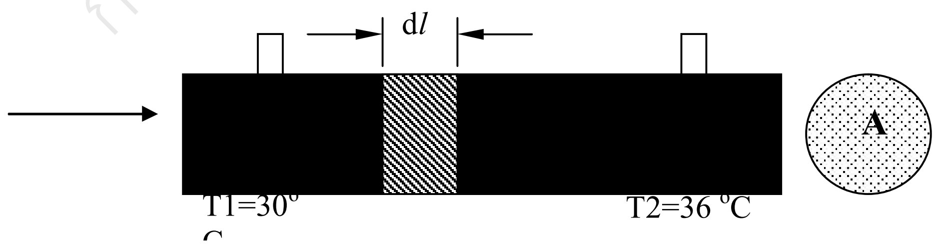

รูปที่ ก-5 ภาพจำลองเซลล์ของระบบเพื่อคำนวณความต้านทานรวมของเซลล์

$$dR = \frac{dl}{\sigma(T).A}$$

(ก.8)

จากสมการ ก.6 จะได้

$$dR = \frac{dl}{(0.0063.T + 0.1330).A}$$

(ก.9)

วิธีหาผลเฉลยของสมการ ก.9 สามารถทำได้หลายวิธีเช่น การหาสมการแม่นตรงโดยใช้สมการ ก.7 ประกอบ การใช้วิธี numerical หรือการประมาณความสัมพันธ์ระหว่างอุณหภูมิกับระยะทาง (Temperature Profile) แต่การหาผลเฉลยแม่นตรง จะมีความซับซ้อน เนื่องจากสมการจะมีรูปแบบที่ยุ่งยาก เพื่อความสะดวกในการหาผลเฉลย ในที่นี้จะทำการประมาณรูปแบบของอุณหภูมิเป็นเชิงเส้นกับระยะทาง จากเงื่อนไขขอบเขต T1=30 ^{o}C และ T2=36 ^{o}C จะได้

$$T = 75.l + 30$$

(ก.10)

จะได้ผลเฉลยดังนี้

$$R_1 = \frac{1}{A}\int_0^{0.08} \frac{dl}{0.4725.l + 0.322}$$

$$R_1 = \frac{0.2349}{A}$$

ในทำนองเดียวกัน จะสามารถคำนวณค่าความต้านทานระหว่างคู่อิเลคโทรดอื่นๆ ได้ดังนี้

$$R_2 = \frac{0.2097}{A}$$

$$R_3 = \frac{0.1867}{A}$$

$$R_4 = \frac{0.1659}{A}$$

$$R_5 = \frac{0.1476}{A}$$

โดยวงจรสมมูลทางไฟฟ้าของเซลล์จะมีความต้านทาน R_1-R_5 ต่อขนานกันอยู่ตามรูปที่ ก-6

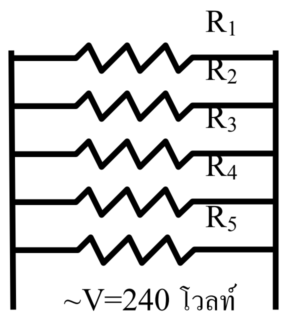

รูปที่ ก-6 วงจรสมมูลทางไฟฟ้าของเซลล์ R1, R2, R3, R4 และ R5 คือความต้านทานในช่วงที่ 1, 2, 3, 4 และ 5 ของเซลล์ตามลำดับ V คือแรงดันตกคร่อมที่ขั้วอิเลคโทรดแต่ละช่วงมีค่าเท่ากับ 240 โวลท์ (สำหรับสนามไฟฟ้า 30โวลท์/เซนติเมตร)

ความต้านทานรวม ΣR มีค่าเท่ากับ $1/\left(\frac{1}{R1}+\frac{1}{R2}+\frac{1}{R3}+\frac{1}{R4}+\frac{1}{R5}\right)$

แทนค่า $A = \pi r^2$

$$\Sigma R = 0.0117 / r^2 \quad (\text{ก}.11)$$

จากข้อกำหนดขนาดของหม้อแปลงที่ออกแบบมีกำลัง 1000 โวลท์-แอมป์ และคิด safety factor 100%

$$P_{\max} = 2.\frac{V^2}{\Sigma R_{\min}} \quad (\text{ก}.12)$$

$$\Sigma R_{\min} = 2.\frac{240^2}{1000} = 115.2\,\Omega \quad (\text{ก}.13)$$

ดังนั้น จะสามารถหาค่ารัศมีของเซลล์ได้โดยสมการ ก.11 และ ก.13

$$r^2 < 0.0117/115.2$$

$$r < 0.01 \text{ m} \quad (\text{ก}.14)$$

เนื่องจากขนาดของท่อควรมีขนาดใกล้เคียงกับอิเลคโทรด เพื่อให้การกระจายสนามไฟฟ้าในตัวอย่างมีความสม่ำเสมอมากที่สุด เมื่อพิจารณาขนาดอิเลคโทรดที่มีขนาดรัศมี 6 มิลลิเมตร ประกอบกับขนาดท่ออคริลิคที่มีในท้องตลาด จึงเลือกขนาดท่ออคริลิคที่มีรัศมี 7 มิลลิเมตรในการทำโอห์มมิคเซลล์แบบต่อเนื่อง รูปที่ ก-7 เป็นรูปโอห์มมิคเซลล์แบบต่อเนื่องที่สร้างขึ้น รูปที่ ก-8 และ ก-9 เป็นอุปกรณ์ต่างๆ ที่ใช้ในระบบให้ความร้อน ส่วนรูปที่ ก-10 เป็นแบบประกอบและแบบรายละเอียดชิ้นส่วนของโอห์มมิคเซลล์แบบต่อเนื่อง

Figure Caption

Figure 1 Schematic diagram of the continuous ohmic heater designed

Figure 2 Model geometry of the heating chamber of the developed continuous ohmic heating system

Figure 3 The continuous ohmic heating system. 1, 2, 9: the supply, recycle and collecting tank, respectively; 3: the screw pump; 4: the ball valve; 5: the continuous ohmic cell; 6: the variable transformer; 7: the digital power meter; 8: the data taker.

Figure 4 Electrical conductivity of 0.02M NaCl Solution.

Figure 5 The remaining proteins in the sample after heating to different temperatures using the continuous ohmic heating system and compared with the result obtained using the batch ohmic heating system (Kanjanapongkul et al, 2007).

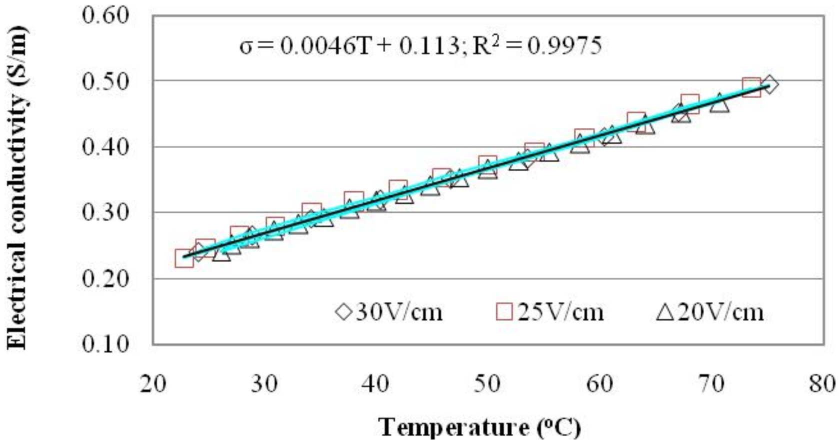

Figure 4 Electrical conductivity of 0.02M NaCl Solution.

Appendix

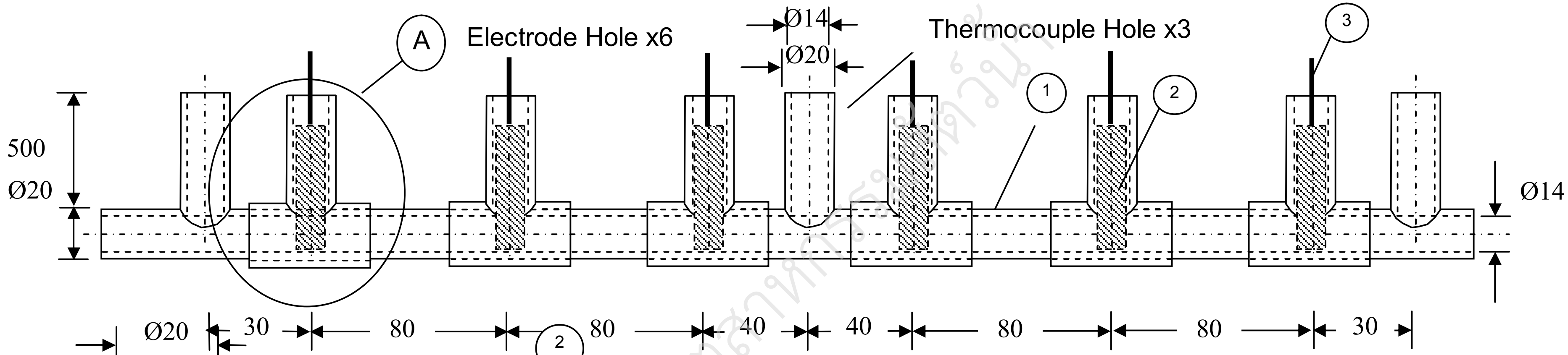

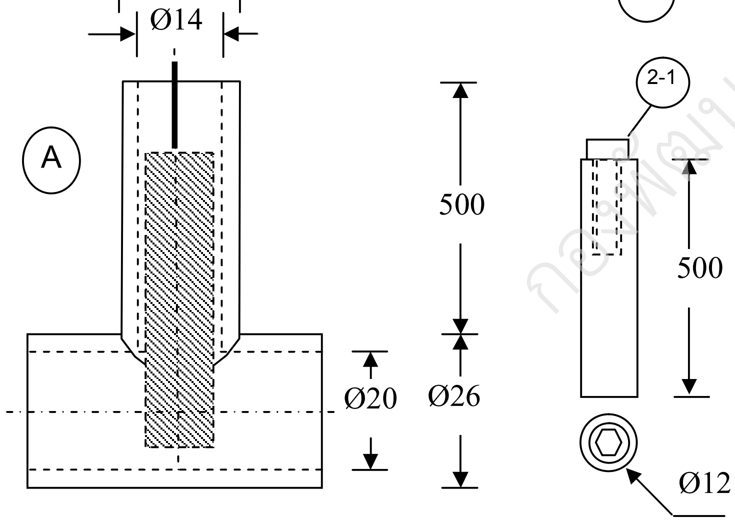

Number	Part Name	Material	Quantity
1	Cell body	Acrylic	1
2	Electrode	Stainless 316	6
2-1	Bolt M6	Stainless	6
3	Wire	Copper	6

Appendix Figure 1: Drawing of Continuous Ohmic Cell and Its Components (in mm)

Example of Calculation by using Numerical method

The 0.02 M NaCl solution was used as example with initial temperature at 27.3°C and the electric field strength of 25 V/cm was applied. The flow rate of the NaCl solution was 300 ml/min. Assumingly, the specific heat of the NaCl solution was constant at 4.1 kJ/kg.°C (Liphard et al., 1976) and its density was approximately 1000 kg/m3. The coefficient a and b obtained from static ohmic experiment in equation (3) were 0.004633 S/m.°C and 0.1126 S/m, respectively. The procedure comprises of 6 steps as following:

1. **Divide the chamber of the continuous ohmic cell into *n* subsections. Thickness of each section, represented by *dz*, is therefore equals to total length of heating section (L) divided by *n*. The electric field strength "E_i" is firstly assumed to be *V/L* for all sections. Then, the model geometry was presented in Figure 2.**

   The continuous ohmic cell internal diameter is 14 mm and was equally divided into 5 sections. Each section was 80 mm long and 6 electrodes located at the intersections.

   The entire ohmic cell, equaled to 400 mm, was divided into 40 equal subsections which was 10 mm long (= 400 mm/40 = 10 mm each subsection). Therefore, the gap between the first couple electrodes could be divided into 8 subsections (=80 mm/10 mm of each subsection).

2. **Estimate the temperature in any incremental section T_{i+1} based on equation (1) by using the following equation:**

$$\frac{\sigma(T_i).(E)^2}{1000} = \rho.C_p.v_z\left(\frac{T_{i+1}-T_i}{dz}\right) \tag{5}$$

   Calculate T1 by firstly, finding the electrical conductivity of the 1st subsection by substituting the initial temperature (T_0) [= 27.3°C] in equation (3)

$$\sigma = a.T + b \tag{3}$$

   Therefore,

$$\sigma(T_0) = 0.0046 * (27.3) + 0.113$$

$$\sigma(T_0) = 0.2391 \qquad \textbf{S/m}$$

Once the inlet temperature of fluid T_0 is known, it is possible to calculate the temperature T_1, T_2, .., T_n. Substitute To = 27.3°C, dz = 0.01 m, E = 3000 V/m (=30 V/cm), Cp = 4.1 kJ/kg.°C, density = 1000 kg/m^3 and Vz =0.02778 m/s into equation (5). The T_1 was obtained which equaled to 27.4312 °C. Repeat the same procedure to calculate T_2, T_3, …, T_{40} for all subsections as following data:

Appendix Table 1: The calculated temperatures of the each subsection

$\mathbf{T_0}$	27.3								
$\mathbf{T_1}$	27.4312	$\mathbf{T_9}$	28.4929	$\mathbf{T_{17}}$	29.5764	$\mathbf{T_{25}}$	30.682	$\mathbf{T_{33}}$	31.8104
$\mathbf{T_2}$	27.5627	$\mathbf{T_{10}}$	28.6271	$\mathbf{T_{18}}$	29.7134	$\mathbf{T_{26}}$	30.8218	$\mathbf{T_{34}}$	31.9531
$\mathbf{T_3}$	27.6946	$\mathbf{T_{11}}$	28.7617	$\mathbf{T_{19}}$	29.8507	$\mathbf{T_{27}}$	30.962	$\mathbf{T_{35}}$	32.0961
$\mathbf{T_4}$	27.8268	$\mathbf{T_{12}}$	28.8966	$\mathbf{T_{20}}$	29.9884	$\mathbf{T_{28}}$	31.1025	$\mathbf{T_{36}}$	32.2395
$\mathbf{T_5}$	27.9593	$\mathbf{T_{13}}$	29.0319	$\mathbf{T_{21}}$	30.1264	$\mathbf{T_{29}}$	31.2434	$\mathbf{T_{37}}$	32.3833
$\mathbf{T_6}$	28.0922	$\mathbf{T_{14}}$	29.1675	$\mathbf{T_{22}}$	30.2648	$\mathbf{T_{30}}$	31.3846	$\mathbf{T_{38}}$	32.5274
$\mathbf{T_7}$	28.2254	$\mathbf{T_{15}}$	29.3035	$\mathbf{T_{23}}$	30.4035	$\mathbf{T_{31}}$	31.5262	$\mathbf{T_{39}}$	32.6719
$\mathbf{T_8}$	28.359	$\mathbf{T_{16}}$	29.4398	$\mathbf{T_{24}}$	30.5426	$\mathbf{T_{32}}$	31.6681	$\mathbf{T_{40}}$	32.8168

The electrical conductivity of each section, σ_i, is obtained using equation (3), and the average temperature value, $(T_i+T_{i-1})/2$ is used in the calculation of σ_i.

3. **Estimate total resistance "R" from the summation of the resistance of each individual section (equation (6)) where the resistance of section i, R_i, is calculated by using equation (7).**

$$R = \sum_{i=1}^{n} R_i \tag{6}$$

$$R_i = \frac{L}{\sigma_i . A} \tag{7}$$

Ri could be calculated by substitute L = 10 mm, A = (22/7)*(7^2 mm^2), and σ_i. from above calculation. Therefore, the resistances of each subsection and summation of resistances of 5 gaps between electrodes could be presented as below table.

Appendix Table 2: The calculated resistances of the each subsection

R1	271	**R9**	266	**R17**	261	**R25**	255	**R33**	250
R2	271	**R10**	265	**R18**	260	**R26**	255	**R34**	250
R3	270	**R11**	265	**R19**	259	**R27**	254	**R35**	249
R4	269	**R12**	264	**R20**	259	**R28**	253	**R36**	248
R5	269	**R13**	263	**R21**	258	**R29**	253	**R37**	248
R6	268	**R14**	263	**R22**	257	**R30**	252	**R38**	247
R7	267	**R15**	262	**R23**	257	**R31**	251	**R39**	246
R8	267	**R16**	261	**R24**	256	**R32**	251	**R40**	246
$\sum \mathbf{R}_{1\text{-}2}$	2152	$\sum \mathbf{R}_{2\text{-}3}$	2108	$\sum \mathbf{R}_{3\text{-}4}$	2066	$\sum \mathbf{R}_{4\text{-}5}$	2025	$\sum \mathbf{R}_{5\text{-}6}$	1984

By $\sum R_{1\text{-}2}$ = total resistance occurred between electrode number 1 and number 2

$\sum R_{2\text{-}3}$ = total resistance occurred between electrode number 2 and number 3

$\sum R_{3\text{-}4}$ = total resistance occurred between electrode number 3 and number 4

$\sum R_{4\text{-}5}$ = total resistance occurred between electrode number 4 and number 5

$\sum R_{5\text{-}6}$ = total resistance occurred between electrode number 5 and number 6

4. Estimate the electric current, "*I*" of each gap, as equation (8) and was showed as following:

$$I = \frac{V}{R} \qquad (8)$$

Appendix Table 3: The calculated currents of the each gap between electrodes

I_{1-2}	0.093
I_{2-3}	0.095
I_{3-4}	0.097
I_{4-5}	0.099
I_{5-6}	0.101

By I_{1-2} = flowing current between electrode number 1 and number 2

I_{2-3} = flowing current between electrode number 2 and number 3

I_{3-4} = flowing current between electrode number 3 and number 4

I_{4-5} = flowing current between electrode number 4 and number 5

I_{5-6} = flowing current between electrode number 5 and number 6

Voltage (Vi) of each subsection could be calculated from multiplying relevant current with the resistance of each subsection. For example, for V1

$$V_1 = I_{1-2} \text{ x } R1 = 0.093 \text{ x } 271 = 25.2 \text{ volt}$$

Therefore, voltage of all 40 subsections is presented below:

Appendix Table 4: The calculated voltages of the each subsection

V_1	25.2	**V_9**	25.2	**V_{17}**	25.2	**V_{25}**	25.2	**V_{33}**	25.2
V_2	25.2	**V_{10}**	25.2	**V_{18}**	25.2	**V_{26}**	25.2	**V_{34}**	25.2
V_3	25.1	**V_{11}**	25.1	**V_{19}**	25.1	**V_{27}**	25.1	**V_{35}**	25.1
V_4	25.0	**V_{12}**	25.0	**V_{20}**	25.0	**V_{28}**	25.0	**V_{36}**	25.0
V_5	25.0	**V_{13}**	25.0	**V_{21}**	25.0	**V_{29}**	25.0	**V_{37}**	25.0
V_6	24.9	**V_{14}**	24.9	**V_{22}**	24.9	**V_{30}**	24.9	**V_{38}**	24.9
V_7	24.8	**V_{15}**	24.8	**V_{23}**	24.8	**V_{31}**	24.8	**V_{39}**	24.8
V_8	24.8	**V_{16}**	24.8	**V_{24}**	24.8	**V_{32}**	24.8	**V_{40}**	24.8

5. Recalculate the electric field strength across each subsection, "E_i", as equation (9)

$$E_i = \frac{I.R_i}{dz} \tag{9}$$

For example, E1 = V1/dz = 25.2 V / 0.01 m = 2520 V/m

Electric field strengths of each subsection were used to recalculate temperatures of each subsection in equation (5), and then recalculate electrical conductivities, resistances, currents, and voltages of each subsection.

6. Repeat step 2-5 until the temperature of each individual subsection converged.

First Calculation

i	z(m)	T_{i-1}	σ	T_i	T_{av}	R_i	$\sum R$	I_i	V_i
1	0.01	27.30000	0.2391	27.43120	27.36560	271.37	2151.77	0.0929	25.2227
2	0.02	27.43120	0.2397	27.56274	27.49697	270.68			25.1588
3	0.03	27.56274	0.2403	27.69461	27.62868	269.99			25.0950
4	0.04	27.69461	0.2409	27.82682	27.76071	269.31			25.0313
5	0.05	27.82682	0.2415	27.95936	27.89309	268.62			24.9679
6	0.06	27.95936	0.2421	28.09224	28.02580	267.94			24.9045
7	0.07	28.09224	0.2428	28.22546	28.15885	267.26			24.8414
8	0.08	28.22546	0.2434	28.35901	28.29223	266.59			24.7784
9	0.09	28.35901	0.2440	28.49291	28.42596	265.91	2108.50	0.0949	25.2227
10	0.10	28.49291	0.2446	28.62714	28.56002	265.24			25.1588
11	0.11	28.62714	0.2452	28.76172	28.69443	264.56			25.0950
12	0.12	28.76172	0.2459	28.89664	28.82918	263.89			25.0313
13	0.13	28.89664	0.2465	29.03190	28.96427	263.22			24.9679
14	0.14	29.03190	0.2471	29.16751	29.09970	262.56			24.9045
15	0.15	29.16751	0.2477	29.30346	29.23548	261.89			24.8414
16	0.16	29.30346	0.2484	29.43975	29.37161	261.23			24.7784
17	0.17	29.43975	0.2490	29.57640	29.50808	260.56	2066.10	0.0968	25.2227
18	0.18	29.57640	0.2496	29.71339	29.64489	259.90			25.1588
19	0.19	29.71339	0.2503	29.85073	29.78206	259.24			25.0950
20	0.20	29.85073	0.2509	29.98842	29.91957	258.59			25.0313
21	0.21	29.98842	0.2515	30.12645	30.05743	257.93			24.9679
22	0.22	30.12645	0.2522	30.26484	30.19565	257.28			24.9045
23	0.23	30.26484	0.2528	30.40358	30.33421	256.62			24.8414
24	0.24	30.40358	0.2535	30.54268	30.47313	255.97			24.7784
25	0.25	30.54268	0.2541	30.68212	30.61240	255.32	2024.55	0.0988	25.2227
26	0.26	30.68212	0.2548	30.82193	30.75203	254.68			25.1588
27	0.27	30.82193	0.2554	30.96208	30.89200	254.03			25.0950
28	0.28	30.96208	0.2560	31.10260	31.03234	253.39			25.0313
29	0.29	31.10260	0.2567	31.24347	31.17303	252.74			24.9679
30	0.30	31.24347	0.2574	31.38470	31.31408	252.10			24.9045

31	0.31	31.38470	0.2580	31.52629	31.45549	251.46			24.8414
32	0.32	31.52629	0.2587	31.66823	31.59726	250.83			24.7784
33	0.33	31.66823	0.2593	31.81054	31.73939	250.19	1983.84	0.1008	25.2227
34	0.34	31.81054	0.2600	31.95321	31.88188	249.55			25.1588
35	0.35	31.95321	0.2606	32.09625	32.02473	248.92			25.0950
36	0.36	32.09625	0.2613	32.23964	32.16795	248.29			25.0313
37	0.37	32.23964	0.2620	32.38341	32.31153	247.66			24.9679
38	0.38	32.38341	0.2626	32.52753	32.45547	247.03			24.9045
39	0.39	32.52753	0.2633	32.67203	32.59978	246.41			24.8414
40	0.40	32.67203	0.2640	32.81689	32.74446	245.78			24.7784

Second Calculation

i	z(m)	T_{i-1}	σ	T_i	T_{av}	R_i	$\sum R$	I_i	V_i
1	0.01	27.30000	0.2391	27.43355	27.36678	271.3611	2151.62	0.0930	25.2239
2	0.02	27.43355	0.2397	27.56677	27.50016	270.6624			25.1589
3	0.03	27.56677	0.2403	27.69966	27.63321	269.9690			25.0945
4	0.04	27.69966	0.2409	27.83221	27.76593	269.2809			25.0305
5	0.05	27.83221	0.2415	27.96442	27.89831	268.5980			24.9671
6	0.06	27.96442	0.2422	28.09630	28.03036	267.9203			24.9041
7	0.07	28.09630	0.2428	28.22784	28.16207	267.2477			24.8415
8	0.08	28.22784	0.2434	28.35905	28.29344	266.5802			24.7795
9	0.09	28.35905	0.2440	28.49534	28.42719	265.9040	2108.35	0.0949	25.2239
10	0.10	28.49534	0.2446	28.63129	28.56331	265.2194			25.1589
11	0.11	28.63129	0.2452	28.76690	28.69910	264.5399			25.0945
12	0.12	28.76690	0.2459	28.90217	28.83454	263.8657			25.0305
13	0.13	28.90217	0.2465	29.03710	28.96964	263.1965			24.9671
14	0.14	29.03710	0.2471	29.17169	29.10440	262.5324			24.9041
15	0.15	29.17169	0.2478	29.30593	29.23881	261.8734			24.8415
16	0.16	29.30593	0.2484	29.43983	29.37288	261.2193			24.7795
17	0.17	29.43983	0.2490	29.57892	29.50937	260.5567	2065.95	0.0968	25.2239
18	0.18	29.57892	0.2496	29.71766	29.64829	259.8858			25.1589

19	0.19	29.71766	0.2503	29.85606	29.78686	259.2201			25.0945
20	0.20	29.85606	0.2509	29.99410	29.92508	258.5594			25.0305
21	0.21	29.99410	0.2516	30.13180	30.06295	257.9037			24.9671
22	0.22	30.13180	0.2522	30.26915	30.20047	257.2529			24.9041
23	0.23	30.26915	0.2528	30.40615	30.33765	256.6071			24.8415
24	0.24	30.40615	0.2535	30.54279	30.47447	255.9662			24.7795
25	0.25	30.54279	0.2541	30.68473	30.61376	255.3170	2024.41	0.0988	25.2239
26	0.26	30.68473	0.2548	30.82632	30.75553	254.6596			25.1589
27	0.27	30.82632	0.2554	30.96756	30.89694	254.0072			25.0945
28	0.28	30.96756	0.2561	31.10844	31.03800	253.3598			25.0305
29	0.29	31.10844	0.2567	31.24896	31.17870	252.7172			24.9671
30	0.30	31.24896	0.2574	31.38913	31.31905	252.0796			24.9041
31	0.31	31.38913	0.2580	31.52894	31.45904	251.4468			24.8415
32	0.32	31.52894	0.2587	31.66839	31.59866	250.8187			24.7795
33	0.33	31.66839	0.2593	31.81325	31.74082	250.1826	1983.70	0.1008	25.2239
34	0.34	31.81325	0.2600	31.95774	31.88549	249.5384			25.1589
35	0.35	31.95774	0.2607	32.10188	32.02981	248.8991			25.0945
36	0.36	32.10188	0.2613	32.24565	32.17376	248.2647			25.0305
37	0.37	32.24565	0.2620	32.38905	32.31735	247.6351			24.9671
38	0.38	32.38905	0.2627	32.53210	32.46058	247.0103			24.9041
39	0.39	32.53210	0.2633	32.67478	32.60344	246.3902			24.8415
40	0.40	32.67478	0.2640	32.81709	32.74593	245.7748			24.7795

Third Calculation

i	z(m)	T_{i-1}	σ	T_i	T_{av}	R_i	$\sum R$	I_i	V_i
1	0.01	27.30000	0.2391	27.43356	27.36678	271.3610	2151.62	0.0930	25.2239
2	0.02	27.43356	0.2397	27.56678	27.50017	270.6623			25.1589
3	0.03	27.56678	0.2403	27.69966	27.63322	269.9689			25.0945
4	0.04	27.69966	0.2409	27.83221	27.76593	269.2809			25.0305
5	0.05	27.83221	0.2415	27.96441	27.89831	268.5980			24.9671
6	0.06	27.96441	0.2422	28.09629	28.03035	267.9203			24.9041
7	0.07	28.09629	0.2428	28.22783	28.16206	267.2478			24.8415
8	0.08	28.22783	0.2434	28.35905	28.29344	266.5802			24.7795

9	0.09	28.35905	0.2440	28.49535	28.42720	265.9040	2108.35	0.0949	25.2239
10	0.10	28.49535	0.2446	28.63131	28.56333	265.2193			25.1589
11	0.11	28.63131	0.2452	28.76691	28.69911	264.5399			25.0945
12	0.12	28.76691	0.2459	28.90218	28.83454	263.8657			25.0305
13	0.13	28.90218	0.2465	29.03710	28.96964	263.1965			24.9671
14	0.14	29.03710	0.2471	29.17168	29.10439	262.5325			24.9041
15	0.15	29.17168	0.2478	29.30592	29.23880	261.8734			24.8415
16	0.16	29.30592	0.2484	29.43983	29.37287	261.2193			24.7795
17	0.17	29.43983	0.2490	29.57893	29.50938	260.5567	2065.95	0.0968	25.2239
18	0.18	29.57893	0.2496	29.71768	29.64830	259.8858			25.1589
19	0.19	29.71768	0.2503	29.85607	29.78687	259.2200			25.0945
20	0.20	29.85607	0.2509	29.99410	29.92509	258.5593			25.0305
21	0.21	29.99410	0.2516	30.13179	30.06295	257.9037			24.9671
22	0.22	30.13179	0.2522	30.26914	30.20046	257.2530			24.9041
23	0.23	30.26914	0.2528	30.40614	30.33764	256.6072			24.8415
24	0.24	30.40614	0.2535	30.54279	30.47446	255.9662			24.7795
25	0.25	30.54279	0.2541	30.68475	30.61377	255.3169	2024.41	0.0988	25.2239
26	0.26	30.68475	0.2548	30.82634	30.75555	254.6595			25.1589
27	0.27	30.82634	0.2554	30.96757	30.89696	254.0071			25.0945
28	0.28	30.96757	0.2561	31.10844	31.03801	253.3597			25.0305
29	0.29	31.10844	0.2567	31.24896	31.17870	252.7173			24.9671
30	0.30	31.24896	0.2574	31.38912	31.31904	252.0796			24.9041
31	0.31	31.38912	0.2580	31.52893	31.45902	251.4468			24.8415
32	0.32	31.52893	0.2587	31.66839	31.59866	250.8188			24.7795
33	0.33	31.66839	0.2593	31.81326	31.74083	250.1825	1983.70	0.1008	25.2239
34	0.34	31.81326	0.2600	31.95776	31.88551	249.5383			25.1589
35	0.35	31.95776	0.2607	32.10189	32.02982	248.8991			25.0945
36	0.36	32.10189	0.2613	32.24565	32.17377	248.2647			25.0305
37	0.37	32.24565	0.2620	32.38905	32.31735	247.6351			24.9671
38	0.38	32.38905	0.2627	32.53209	32.46057	247.0103			24.9041
39	0.39	32.53209	0.2633	32.67477	32.60343	246.3903			24.8415
40	0.40	32.67477	0.2640	32.81709	32.74593	245.7748			24.7795

Fourth Calculation

i	z(m)	T_{i-1}	σ	T_i	T_{av}	R_i	$\sum R$	I_i	V_i
1	0.01	27.30000	0.2391	27.43356	27.36678	271.3610	2151.62	0.0930	25.2239
2	0.02	27.43356	0.2397	27.56678	27.50017	270.6623			25.1589
3	0.03	27.56678	0.2403	27.69966	27.63322	269.9689			25.0945
4	0.04	27.69966	0.2409	27.83221	27.76593	269.2809			25.0305
5	0.05	27.83221	0.2415	27.96441	27.89831	268.5980			24.9671
6	0.06	27.96441	0.2422	28.09629	28.03035	267.9203			24.9041
7	0.07	28.09629	0.2428	28.22783	28.16206	267.2478			24.8415
8	0.08	28.22783	0.2434	28.35905	28.29344	266.5802			24.7795
9	0.09	28.35905	0.2440	28.49535	28.42720	265.9040	2108.35	0.0949	25.2239
10	0.10	28.49535	0.2446	28.63131	28.56333	265.2193			25.1589
11	0.11	28.63131	0.2452	28.76691	28.69911	264.5399			25.0945
12	0.12	28.76691	0.2459	28.90217	28.83454	263.8657			25.0305
13	0.13	28.90217	0.2465	29.03709	28.96963	263.1965			24.9671
14	0.14	29.03709	0.2471	29.17168	29.10438	262.5325			24.9041
15	0.15	29.17168	0.2478	29.30592	29.23880	261.8734			24.8415
16	0.16	29.30592	0.2484	29.43983	29.37287	261.2193			24.7795
17	0.17	29.43983	0.2490	29.57893	29.50938	260.5567	2065.95	0.0968	25.2239
18	0.18	29.57893	0.2496	29.71768	29.64830	259.8858			25.1589
19	0.19	29.71768	0.2503	29.85607	29.78687	259.2200			25.0945
20	0.20	29.85607	0.2509	29.99410	29.92508	258.5593			25.0305
21	0.21	29.99410	0.2516	30.13179	30.06295	257.9037			24.9671
22	0.22	30.13179	0.2522	30.26914	30.20046	257.2530			24.9041
23	0.23	30.26914	0.2528	30.40613	30.33763	256.6072			24.8415
24	0.24	30.40613	0.2535	30.54279	30.47446	255.9662			24.7795
25	0.25	30.54279	0.2541	30.68475	30.61377	255.3169	2024.41	0.0988	25.2239
26	0.26	30.68475	0.2548	30.82634	30.75554	254.6595			25.1589
27	0.27	30.82634	0.2554	30.96757	30.89696	254.0071			25.0945
28	0.28	30.96757	0.2561	31.10844	31.03801	253.3597			25.0305
29	0.29	31.10844	0.2567	31.24896	31.17870	252.7173			24.9671

30	0.30	31.24896	0.2574	31.38912	31.31904	252.0796			24.9041
31	0.31	31.38912	0.2580	31.52893	31.45902	251.4468			24.8415
32	0.32	31.52893	0.2587	31.66839	31.59866	250.8188			24.7795
33	0.33	31.66839	0.2593	31.81326	31.74082	250.1825	1983.70	0.1008	25.2239
34	0.34	31.81326	0.2600	31.95776	31.88551	249.5383			25.1589
35	0.35	31.95776	0.2607	32.10189	32.02982	248.8991			25.0945
36	0.36	32.10189	0.2613	32.24565	32.17377	248.2647			25.0305
37	0.37	32.24565	0.2620	32.38905	32.31735	247.6351			24.9671
38	0.38	32.38905	0.2627	32.53209	32.46057	247.0103			24.9041
39	0.39	32.53209	0.2633	32.67477	32.60343	246.3903			24.8415
40	0.40	32.67477	0.2640	32.81709	32.74593	245.7748			24.7795